Electronic Supplementary Material (ESI) for Biomaterials Science.

Electronic Supporting Information

Mechanical Behavior of Biomimetic Oriented Cell Sheets from a Perspective of Living Materials

Wei Xu,[a] Shuangshuang Chen,*[b] Mengting Yao [c] and Qinghua Lu *[ac]

[a]School of Chemistry and Chemical Engineering, Frontiers Science Center for Transformative Molecules, the State Key Laboratory of Metal Matrix Composites, Shanghai Jiao Tong University, Shanghai, 200240 China;

[b]Institute of Translational Medicine, Shanghai University, Shanghai, 200444 China;

[c]School of Chemical Science and Engineering, Tongji University, Shanghai, 200092 China

*Email: fjchenss@sjtu.edu.cn; qhlu@sjtu.edu.cn

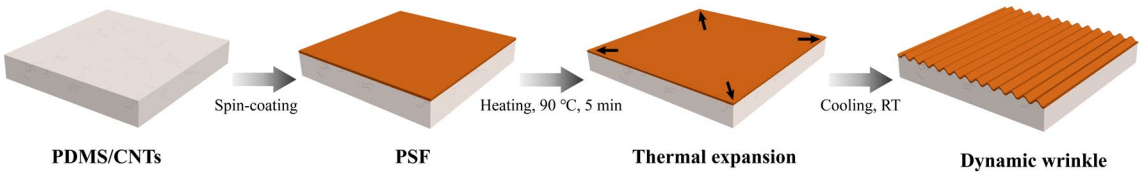

Figure S1. A schematic representation of the near-infrared (NIR)-triggered thermomechanical dynamic wrinkle layer.

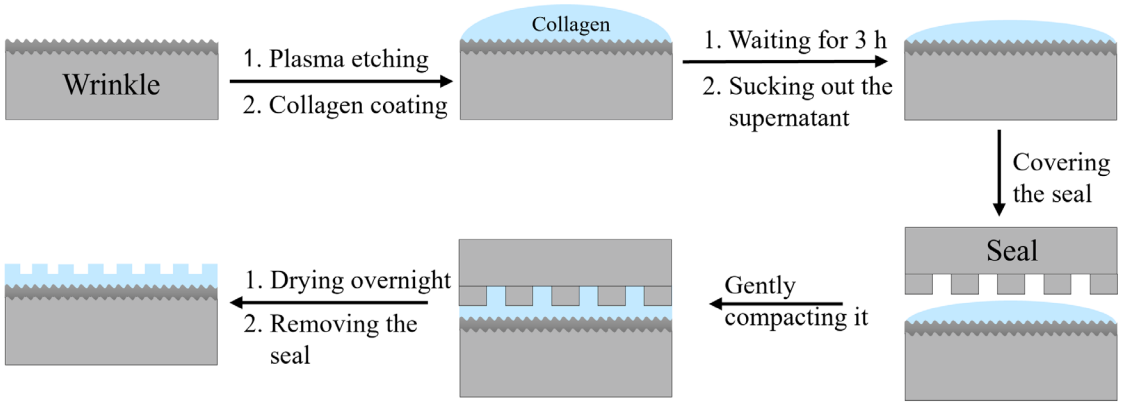

Figure S2. The preparation of patterned substrates containing an array of parallel grooves.

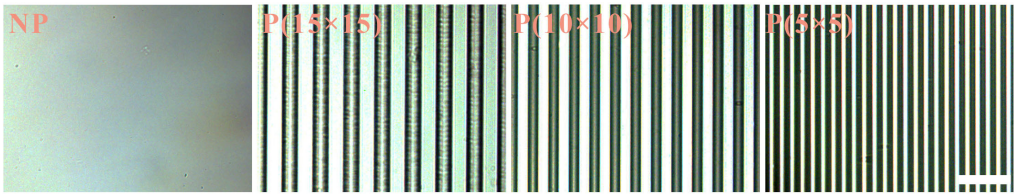

Figure S3. Optical images of the non-patterned (NP) and patterned (P) collagen layers. Scale bar = 50 μm.

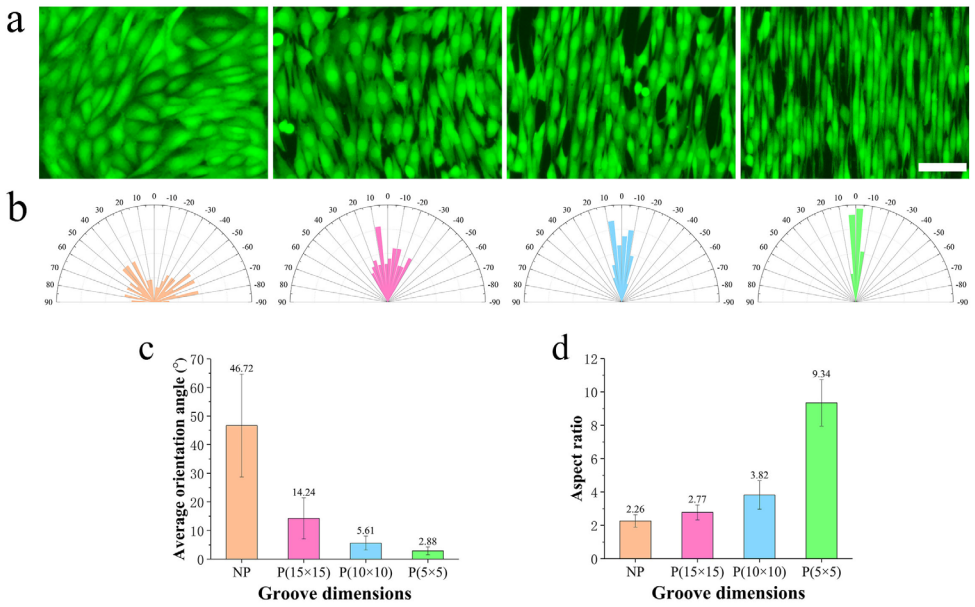

Figure S4. The effect of the microgrooves on cell alignment: (a) Fluorescence images of cells grown on non-patterned (NP) and patterned (P) collagen layers and stained with calcein-AM. (b) The distribution of the average orientation angle (°) between the long axis of cells and the direction of the grooves. (c) The average orientation angles between the long axis of cells and the direction of the grooves. (d) Aspect ratio of the cells. Scale bar = 50 μm.

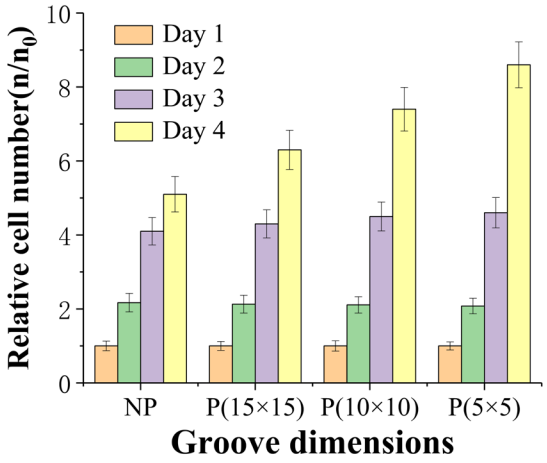

Figure S5. The number of cells on non-patterned (NP) and patterned (P) collagen layers. The relative cell number represents the ratio of real-time cell number (n) to initial cell number (n_0).

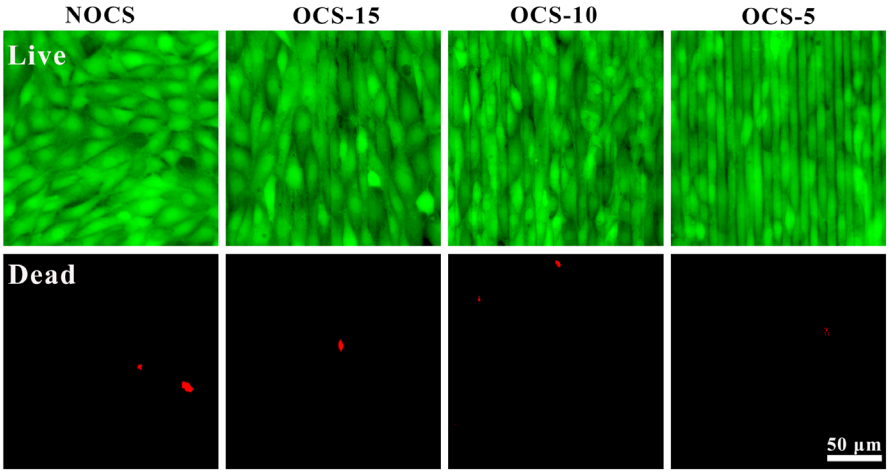

Figure S6. Fluorescence images of the cell viability on the random cell sheets (NOCSs) and oriented cell sheets (OCS-15, 10 and 5) using calcein-AM/PI staining.

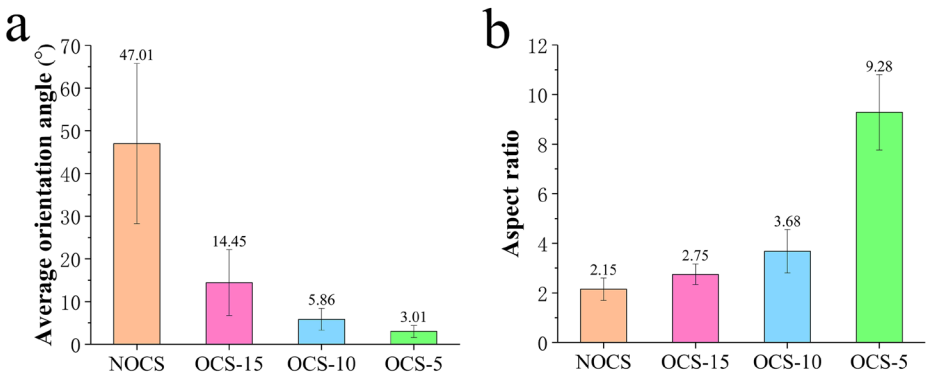

Figure S7. The cellular orientation of the harvested cell sheets. (a) The average orientation angles between the long axis of cells and the direction of the grooves. (b) The cellular aspect ratio of the random cell sheets (NOCS) and oriented cell sheets (OCS-15, 10 and 5).

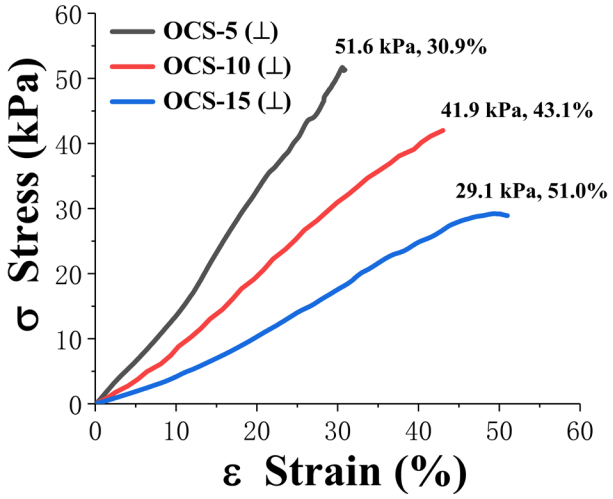

Figure S8. The stress-strain curves for OCSs (-15, -10 and -5) in the perpendicular direction to the cell alignment.

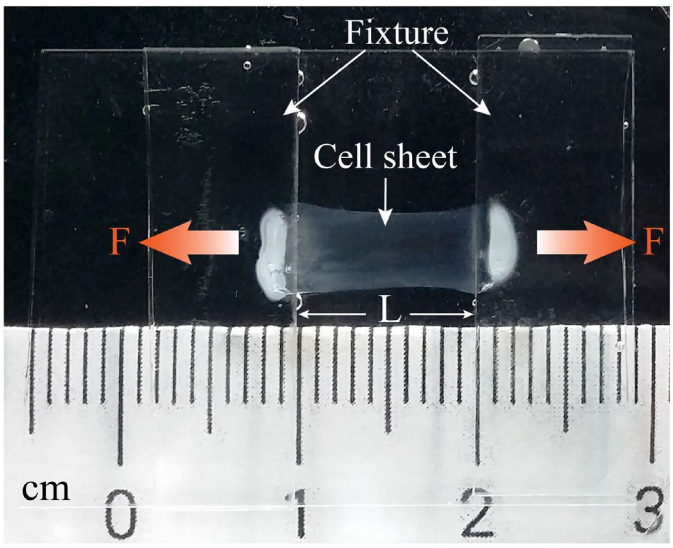

Figure S9. The homemade apparatus with two fixtures used to hold the cell sheet during in-situ stretching. The apparatus was used in PBS and could be placed onto an objective table of a microscope for in-situ observation.

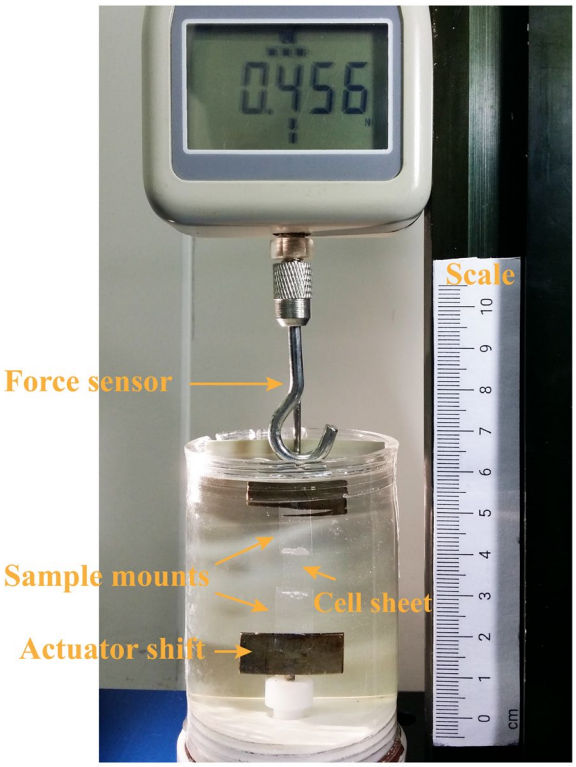

Figure S10. The homemade apparatus used for mechanical relaxation testing. The strains of cell sheet were set at 5 and 25%, respectively. The stress was recorded using a digital force gauge (Yilida, China).

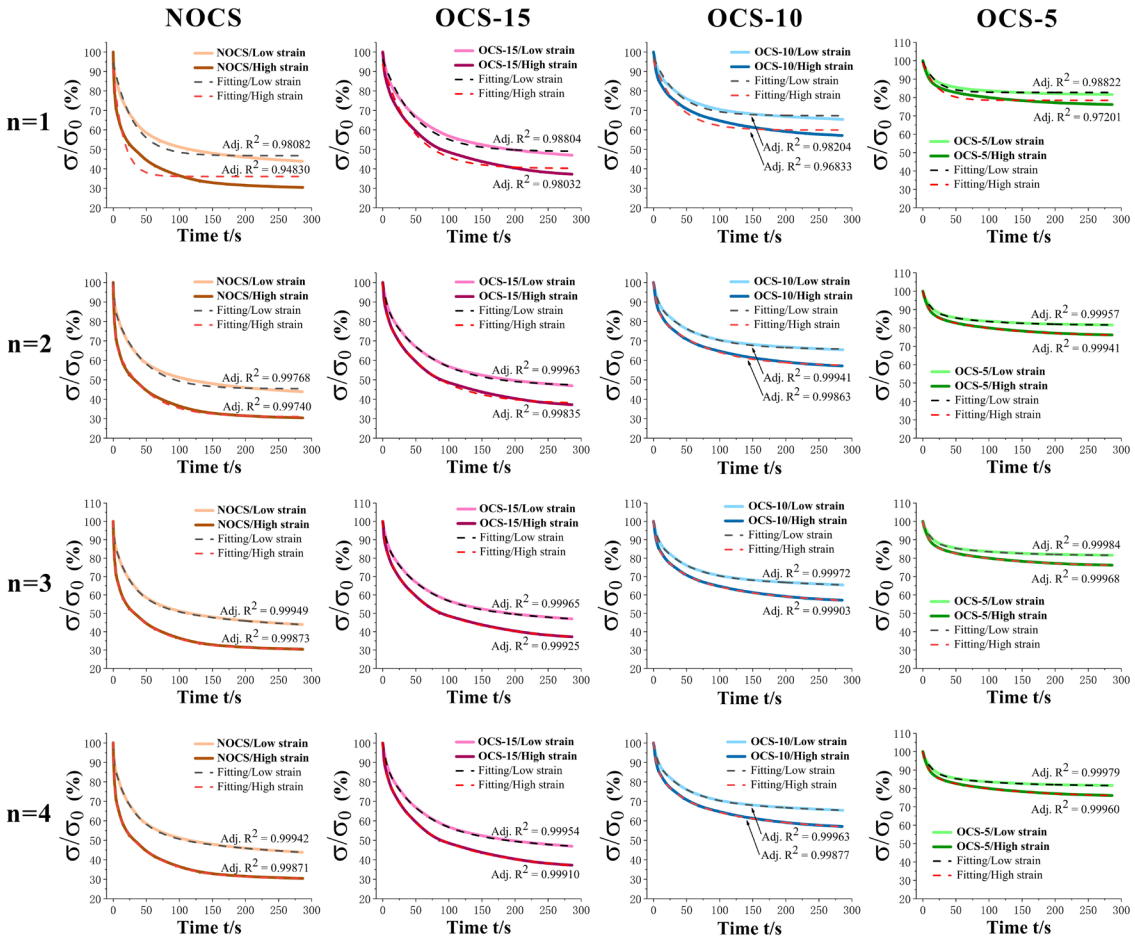

Figure S11. The fitting curves obtained for the stress relaxation data using the Maxwell–Wiechert model (n). The Maxwell–Wiechert model (n = 3) was used to fit the stress relaxation curves of the cell sheets in the low and high strain regions.

Table S1. The adjusted coefficient of determination (Adj. R^2) of the fitting curves obtained for the oriented cell sheets based on the Maxwell–Wiechert model (n).

Adj. R^2	NOCS		OCS-15		OCS-10		OCS-5	
	Low strain	High strain	Low strain	High strain	Low strain	High strain	Low strain	High strain
n=1	0.98082	0.94830	0.98804	0.98032	0.98204	0.96833	0.98822	0.97201
n=2	0.99768	0.99740	0.99963	0.99835	0.99941	0.99863	0.99957	0.99941
n=3	0.99949	0.99873	0.99965	0.99925	0.99972	0.99903	0.99984	0.99968
n=4	0.99942	0.99871	0.99954	0.99910	0.99963	0.99877	0.99979	0.99960

Table S2. Fitting parameters for the stress relaxation data using the Maxwell–Wiechert model (n = 3).

Types	A_∞ (%) (mean ± s.d.)	A_1 (%) (mean ± s.d.)	A_2 (%) (mean ± s.d.)	A_3 (%) (mean ± s.d.)	τ_1 (s) (mean ± s.d.)	τ_2 (s) (mean ± s.d.)	τ_3 (s) (mean ± s.d.)	Adj. R^2
NOCS-L	41.62 ± 2.389	31.24 ± 4.710	17.33 ± 3.113	9.66 ± 0.709	25.53 ± 3.750	141.25 ± 74.552	1.18 ± 0.184	0.99949
NOCS-H	30.41 ± 0.621	35.06 ± 1.826	22.61 ± 2.425	12.26 ± 2.852	124.50 ± 5.311	34.62 ± 1.154	2.60 ± 0.198	0.99873
OCS15-L	46.68 ± 0.021	25.50 ± 2.392	14.87 ±3.598	8.41 ± 1.687	26.84 ±2.650	146.05 ± 10.527	2.01 ± 0.494	0.99965
OCS15-H	33.45 ± 3.932	28.35 ± 8.891	20.69 ± 11.584	11.74 ± 1.321	139.47 ± 6.190	32.22 ± 1.453	2.31 ± 0.421	0.99925
OCS10-L	64.32 ± 3.576	15.11 ± 2.425	10.71 ± 0.569	6.42 ± 0.768	28.47 ±2.386	137.05 ± 7.257	1.87 ± 0.637	0.99972
OCS10-H	53.92 ± 4.426	18.98 ± 6.043	12.45 ± 8.522	7.10 ± 2.101	140.47 ± 139.802	30.81 ± 8.653	3.70 ± 0.753	0.99903
OCS5-L	81.27 ± 0.152	9.51 ± 0.351	6.46 ± 0.346	1.76 ± 0.247	19.76 ± 0.771	123.50 ± 10.274	1.25 ± 0.621	0.99984
OCS5-H	75.26 ± 0.461	11.15 ± 1.197	9.41 ± 0.699	4.06 ± 1.472	111.83 ± 12.677	27.45 ± 4.968	4.42 ± 1.073	0.99968

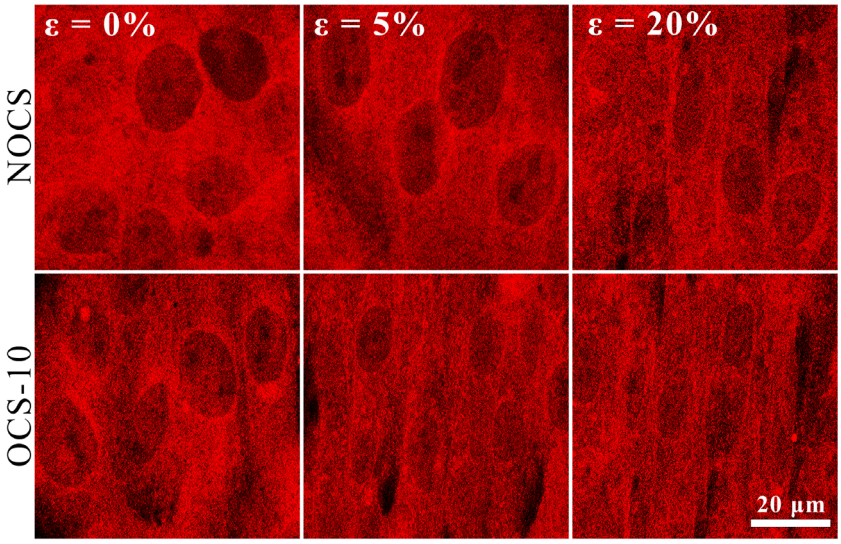

Figure S12. Fluorescence images after N-cadherin staining of the cell sheets (NOCSs and OCS-10) during stretching.

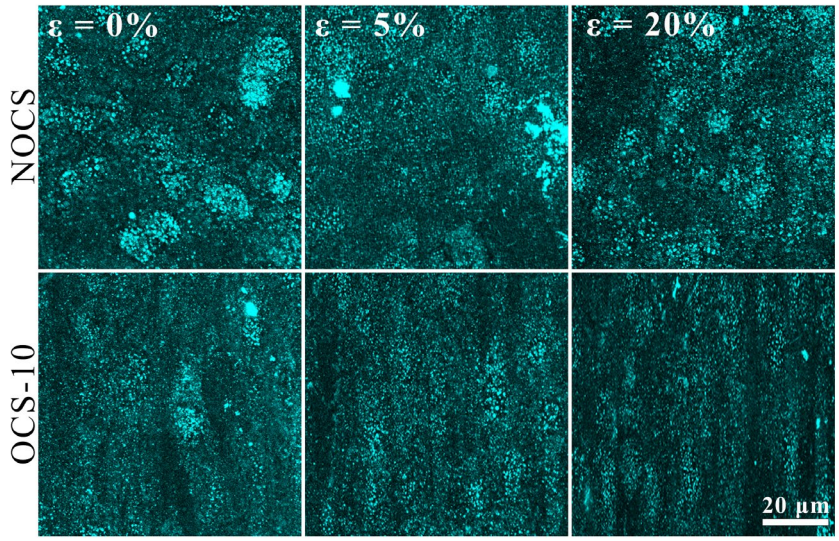

Figure S13. Fluorescence images after collagen(VI) staining of the cell sheets (NOCSs and OCS-10) during stretching.